AFM and SEM assessment of lubricating grease microstructures: influence of sample preparation protocol, frictional working conditions and composition

C. Roman, C. Valencia, J. M. Franco✉

Chemical Process and Product Technology Research Center (Pro²TecS).

Dept Ingeniería Química Campus de 'El Carmen', Universidad de Huelva. 21071 Huelva. Spain.

✉ Author to whom correspondence should be addressed:

E-mail address: franco@uhu.es.

Tel.: +34959219995

Fax: +34959219983

Abstract

The microstructure of lubricating greases greatly conditions their in-service performance. In that sense, optimal testing protocols are required in order to accomplish their correct morphological characterization. This study explores and compares the suitability of Atomic Force Microscopy (AFM) and Scanning Electron Microscopy (SEM) techniques for imaging six different commercial metallic soap-based greases and two novel biopolymer-based formulations. Pros and cons of both techniques as well as the effect of sample preparation protocol were analyzed. The results revealed a wide variety of morphological characteristics depending on composition. Thus, the four anhydrous calcium-based greases demonstrated two clearly distinct microstructures (fibrous and granular) determined by the type of base oil employed. With regard to the lithium complex greases, the typically reported microstructure characterized by well-defined entangled and fibrous network was observed in both AFM and SEM techniques. As for the two biopolymer-based greases, fiber networks were also encountered. Besides this, selected greases were subjected to different tribological tests, and the effect of high-shear frictional working treatments on their microstructure was also analyzed. As a result of the friction and internal wear, the AFM results evidenced microstructural changes which depended on grease composition. Overall, the combined use of AFM and SEM techniques was demonstrated to be a powerful approach to microstructurally characterize lubricating greases.

Keywords: AFM; SEM; lubricating grease; microstructure; friction

1. Introduction

Nowadays, lubricating greases are of utmost importance for both a wide variety of industrial applications and everyday lubrication challenges as they are designed to maximize efficiency and prolong the useful service life of all moving equipment [1]. In general, the design and development of lubricants require ample experience and knowledge to obtain an appropriate behavior for specific applications. In the particular case of lubricating greases, further adequate microstructure and related physical properties must be reached from an appropriate sequence selection of both grease ingredients and manufacturing process [2, 3].

Lubricating greases are essentially highly-structured two-phase colloidal suspensions consisting of a thickening agent, usually a metal soap, such as lithium, sodium and calcium salts of long chain fatty acids, dispersed in a lubricating liquid such as mineral, synthetic or vegetable-derived oils. The thickener forms a three-dimensional gelling network which traps the oil and confers the appropriate rheological and tribological behavior to the grease [4, 5]. These particular rheological characteristics imparted by the thickener make lubricating greases more convenient in some applications where lubricating oils do not work properly, like rolling bearings. Actually, factors like decreasing leakage and frequency of lubrication in hard-to-reach contacts, fluctuations with temperature, loads, vibrations, etc. can be minimized when using greases [6]. Apart from the main lubrication role, which is mainly performed by the lubricating oil, the rest of differential and characteristic performance properties of lubricating greases are due to the microstructure. Several authors have highlighted the role of the thickener in film thickness [7-10], some of them emphasizing the thickener microstructure [11]. Recently, Cyriac et al. [12] pointed out in a very elucidating work the importance of grease microstructure on the lubrication film thickness, demonstrating that the smaller thickener structural units, the thicker films were obtained. Hence, acquiring new knowledge and understanding on how the microstructure of grease thickener can provide functional properties for both, good lubrication performance and lifetime is essential.

Microscopy methods like atomic force microscopy (AFM), scanning electron microscopy (SEM) or transmission electron microscopy (TEM), reveals micro- and nanoscale structural details, and therefore are powerful and effective tools for visualising the lubricating grease morphology [13-18]. However, in spite of the continual development and great diversity of microscopy techniques, microstructure determination of lubricating greases remains a current challenge. This is because most electron microscopy methods are based on observations of thin sections or surfaces that show a cross-section of the structure. Besides that, some surface topographies of soft specimens could be affected by the sample preparation/treatment method [19].

Despite the fact that there is a rather extensive literature describing the use of TEM and SEM techniques to investigate the grease microstructure [13, 14, 16, 20], the two techniques present some drawbacks. Both of them are vacuum based and, therefore the oil component must be removed or its volatility reduced before analysis, for instance by freezing the sample. The most common criticism associated to SEM and TEM analysis is that these techniques can alter the original grease microstructure [14, 16, 21] as a result of modifying the thickener-oil interaction balance. For instance, much more agglomerated structural units have been observed using the SEM technique in washed samples than those observed in non-washed samples using the AFM technique [12].

Taking into account that greases may contain large amount of lubrication oil, one of the main goals in this study was to establish a reliable method to observe the thickener microstructure of different lubricating greases by preserving the integrity of the samples as much as possible. In particular, since the AFM can work in various environments (vacuum, air and liquid), many researchers have been interested in imaging soft or biological samples [22, 23]. Furthermore, recent advances in AFM have enabled high-speed imaging of soft samples allowing the direct visualization of biomolecules [24, 25]. So far, some specific observations of grease microstructures by means of atomic force microscopy have been previously reported [12, 15, 18, 26-29]. However, it still remains difficult to image the nanoscale topography of lubricating grease samples by AFM, because some artifacts can arise due to non-desired interactions between the tip and the sample as a consequence of several factors such as tip geometry, lateral forces or grease textural and rheological properties. For instance, soft greases having low consistency can induce the sticking of the tip to the sample and consequently, the AFM image on the specimen microstructure can show artefacts or cannot be obtained. In this sense, Hurley and Cann [11] were not able to obtain good observations in non-washed samples using the contact mode. Some of these problems can be avoided by heating the grease sample below the dropping point and then cooling down to obtain smooth enough films [18, 26, 27]. However, this pre-heating protocol must be also optimized to avoid any change in the thickener-oil interaction balance. In spite of the mentioned limitations, this technique provides great advantages, as the microstructure analysis can be performed under atmospheric pressure and enables to visualize surface microstructure in almost non-perturbed grease samples.

Taking into account these considerations, this work aims to investigate the topography (surface features) and morphology (overall shape) of different lubricating greases, including several commercial samples with different composition and some novel biopolymers-based grease formulations, by means of SEM and AFM techniques and compare the information that can be derived from both techniques. The pre-heating protocol to obtain accurate AFM observations on non-washed samples was optimized. In addition, the effect of high-shear working treatments on lubricating grease microstructure in some tribological tests was also explored on selected samples.

2. Experimental

2.1. Materials

Eight lubricating grease samples differing on their composition were analysed from a microstructural point of view. Samples C1-C6 were commercially available calcium and lithium soap-based greases whereas biopolymer-based model samples M1 and M2 were manufactured in the laboratory as described elsewhere [29, 30]. Compositional details of the different lubricating greases analysed in this study as well as basic properties are listed in Table 1. The selection of grease samples was done according to the different compositional variables aimed to be studied, i.e. type of thickener and type and viscosity of base oil.

2.2. AFM observations

Morphological observations of grease samples were investigated using a multimode AFM connected to a Nanoscope IV scanning probe microscope controller (Digital Instruments, Veeco Metrology Group Inc., Santa Barbara, CA) using the tapping mode with phase detection imaging at room temperature. Tapping mode amplitude modulation microscopy is an adequate approach for imaging soft materials such as lubricating greases because it involves the repeated oscillation of the cantilever at or slightly below its resonant frequency. The amplitude of oscillation typically ranges from

20 nm to 100 nm. The tip lightly interacts with the sample surface during scanning providing high resolution images with minimum sample damage. Silicon Nanosensors™ PPP-NCH AFM probes for tapping mode with a force constant of 42 N/m and resonance frequency of 330 kHz were used. Scan speed was set at 1 Hz and scan windows were taken from 5 to 20 μm.

In order to obtain good imaging quality the specimens for AFM examination require an appropriate preliminary preparation. Grease sample preparation for accurate observations is one of the most challenging and essential steps in AFM microstructural analysis because of the grease low consistency. A pre-heating treatment at a temperature below the dropping point of the lubricating grease was applied in order to form a smooth surface which yields a good resolution. A MR Hei Standard hotplate from Heidolph was used for heating grease samples. Different time-temperature combinations comprised between 100 ºC and 240 ºC for 5-30 s were tested depending on the sample. The optimized time-temperature procedures established for each sample are included in Table 2. Afterwards, samples were cooled down to room temperature for some minutes before placing them in the AFM holder and starting the scan sequence. In the particular case of sample C4, accurate observations were only feasible without heating the sample.

2.3. SEM observations

The morphological analysis of the lubricating greases by means of scanning electron microscopy (SEM) was performed in a JEOL microscope (Japan), model JSM-5410, operating at 15 and 20 kV accelerating voltages. This scanning electron microscope covers the practical magnification range from 200X to 13 000X.

Since SEM requires a hard vacuum in the sample chamber, the extraction of oil was absolutely necessary to image the sample morphology. In the process of SEM analysis, preliminary treatment of the lubricating grease is one of the most time consuming steps. The goal of extraction process is effective isolation of the thickener agent from the matrix by use of a non-polar organic solvent with minimal effect on specimens. Hence, oil was extracted by immersing the sample for one week in n-hexane. The solvent was carefully replaced 3 - 4 times per day, until oil extraction was completed. Afterwards, the samples were stored and dried at room temperature for a period of some days until ready for use. Moreover, as conventionally done, in order to prevent charging of the surface, reduce thermal damage and improve the secondary electron signal required for topographic examination in the SEM, the samples were coated with a thin layer of gold by means of a sputter coater HHV Scancoat Six SEM.

2.4. Tribological measurements

Three selected greases (C5, C6 and M1) were used as lubricants in a tribological contact in order to evaluate the effect of a severe working treatment on grease microstructure. Samples were placed in a tribological cell coupled with a controlled-stress rheometer, Physica MCR-501 (Anton Paar, Austria), as described elsewhere [30]. At least three replicates of each test were performed at room temperature on fresh samples and resulting worked grease samples were analyzed by AFM. Tribological test conditions are collected in Table 3.

3. Results and Discussion

3.1. Influence of sample preparation protocol

The influence of the pre-heating treatment on AFM imaging lubricating grease microstructures was analysed on samples C5, a lithium complex-based grease, and C6, a lithium-calcium complex grease. Figure 1 shows selected AFM micrographs of these samples obtained after applying different pre-heating temperatures and times. As can be observed, there are significant microstructural similarities between the same samples as long as the applied temperature was well below the dropping point of the grease and the heating time was not longer than typically 15-30 s. However, the time-temperature combination which produces significant changes in the microstructure depends on grease consistency and thickener type.

It can also be noticed that the typical entangled fibrous microstructure is apparent in sample C5 when heating at 200 ºC for 30 s, where long and twisted individual fibres can be detected. AFM phase micrographs still display the lithium soap thickener in the form of highly entangled but slightly more agglomerated fibre network when pre-heating the sample at 210 ºC for 15 s. However, much more agglomerated fibres and compact structure can be visualized at 225 ºC.

Regarding sample C6, the lithium-calcium complex thickener forms a connecting fibrous-granular microstructure, where the calcium soap appears dispersed and homogeneously distributed in the form of granules of around 0.5 μm in a fibrous network, which can be roughly observed by pre-heating the sample at 200 ºC. The same microstructure can be visualized with better resolution by pre-heating the sample at 225 ºC. However, after heating at 240 ºC, rather close to the dropping point (see Table 1), a significant change in the microstructure can be clearly detected. The lithium soap thickener appears like shorter and less intricate fibres network while the calcium soap thickener remains dispersed in the grease matrix in form of larger spherical granules, with sizes of around 2-4 μm. This increase in diameter of the calcium granules for sample C4 could be attributed to a partial melting of the calcium thickener and further re-crystallization. Furthermore, the base oil could evaporate at the surface producing the agglomeration of thickener particles. These results strongly suggest that it is essential to determine the right time-temperature procedure before AFM imaging a specific lubricating grease. In the next sections, AFM images obtained after optimizing the pre-heating protocol are shown. The optimization of this pre-heating treatment dealt with the application of different time-temperature combinations, in the ranges shown in Table 2 for each specific grease, and the evaluation of the resulting microstructure. Typically, the higher temperature and/or heating time, the higher resolution was found. The optimum time-temperature combinations were considered those providing the higher image resolution without inducing any significant microstructural change compared to the non-heated or just slightly heated microstructure.

3.2. Comparison between AFM and SEM imaging of lubricating grease microstructures

Although grease sample preparation for SEM and AFM imaging is really different, actually they are complementary techniques. Thus, the AFM is adequate technique at measuring surface height of the almost unperturbed sample, often at extremely high resolution, while the SEM provides elemental analysis of the surface by detecting sharp changes in height or slope of the thickener skeleton. Furthermore, one technique often compensates for the imaging artefact of the other [31].

AFM and SEM techniques were used to examine the eight different lubricating grease samples studied and actually similar microstructures were obtained. In general, two main distinct types of thickener structure (fibrous and/or granular) were possible to observe in both AFM and SEM micrographs. The AFM images reported in this section were performed by using the tapping mode in phase imaging once considered the optimum time-temperature sample preparation procedure which was previously determined (see Table 2).

Figures 2-4 show a comparison between the phase images taken by AFM and SEM micrographs for the different lubricating greases studied. The two techniques present different principles of operation and therefore the micrographs are presented in different arrangements and window sizes. However, it is evident that all microstructures determined by AFM are quite similar to those obtained by SEM analysis, which demonstrates that oil extraction does not exert a great influence in the thickener arrangement, at least from a qualitative point of view. Thus, the main difference observed between the two sets of images is that SEM microstructures seem to appear more agglomerated and collapsed as a consequence of oil removing. In a few cases, the structural units are not easily detectable as a result of this collapse (see for instance Figure 2, sample C4, and Figure 4, sample M2). Figure 2 shows different anhydrous calcium soap microstructures formed in different oil media. Taking into account that all samples are anhydrous calcium-based greases, completely different microstructures of the soap thickener can be observed in both AFM and SEM analysis. Thus, the microstructure of samples C1 and C4 consist of fine, small and slightly entangled and twisted fibres as previously described [13,32], whereas a granular and/or sponge-like thickener microstructure was detected in both AFM and SEM micrographs for samples C2 and C3, when the thickener was dispersed in vegetable-derived oils. However, a certain degree of crosslinked structures can be distinguished for sample C2 in the SEM image taken at the highest magnification (Figure 2). On the other hand, a well-formed, twisted and tangled fibrous network with thicker fibres but more agglomerated can be detected by SEM operating with 20 kV accelerating voltage and 1000X-1200X magnification for samples C1 and C4.

The typical twisted and tangled fibrous arrangements of lithium greases were observed in sample C5 (Figure 3) using both AFM and SEM techniques. Due to the interactions between these colloidal particles and oil phase, these fibres have the ability to arrange themselves into a specific fibrous microstructure. This characteristic lithium soap arrangement is more evident in AFM images where the oil is present.

Concerning sample C6, the above discussed characteristic mixed structure, where the lithium soap thickener appears distributed in a random manner in form of short and dense fibres and the calcium soap thickener remains dispersed in the grease matrix in form of spherical granules, was evidenced. Inspection of AFM images in Figure 3 reveals a quite complex phase behaviour of the two metallic soaps with the capacity to perfectly immobilise the base oil. This particular microstructure is the most affected by oil removing. However, still using the SEM technique it was possible to observe the same structural network of granules dispersed in a fibrous structure (Figure 3).

Finally, Figure 4 shows selected AFM and SEM images of the two model biopolymer-based greases used in this study. In the case of both samples, M1 and M2, it was possible to observe a quite dense and tangled fibrous network which very much resembles a lithium soap microstructure. Much finer and shorter fibres were observed in the microstructure provided by the chemically modified methylcellulose (M1) using the AFM technique. The fibres structure is also easily detectable in SEM images for sample M1, although at different scale. However, the long and twisted fibres observed with AFM in the lignocellulosic material-based grease (sample M2) were not really well appreciated by SEM analysis, where only at 1000X magnification a fibrous structure can be guessed.

3.3. Influence of compositional variables

As can be deduced from the microscopy observations previously discussed, the morphology of grease structure greatly depends on the composition, both type of thickener and base oil. The typical morphologies given by the most common thickener agents have been previously reported [4,13-15,18]. However, the influence of either the base oil or the interaction between the base oil and the thickener has not still been investigated in detail. Most widely used thickening agents in grease formulations are fatty acid soaps of lithium and calcium. The AFM and SEM images of three different calcium (C1), lithium (C5), and lithium-calcium (C6) thickening agents dispersed in a mineral oil are compared (see Figures 1 and 2). Presuming similar hydrophobic interactions between the mineral base oil and the fatty acid soaps, the different morphologies are essentially due to the typical crystallization patterns of each fatty acid soap. Microstructures of anhydrous and lithium complex soaps encountered in this study are in agreement with those previously reported in the literature taken by SEM and TEM analysis [13-16]. Relatively short, thin and not especially agglomerated fibres can be observed by means of AFM analysis in the case of grease C1. This sample was difficult to image after pre-heating by means of AFM due to an excessive softening of the sample. This behaviour is particularly associated with a low viscosity of the base oil (see Table 1). Hence, greases containing a low-viscosity base oil or high content of oil, i.e. soft greases, may give poor images and some artefacts during scanning due to contamination of the AFM-tip by the oil. The entangled fibrous structure of the anhydrous calcium-based grease examined (C1) can be also observed in Figure 2 by SEM. With regard to the lithium complex grease (sample C5), the typical fibrous and entangled microstructure was observed in both AFM and SEM techniques (see Figure 3). Finally, in the case of sample C6, as previously discussed, Figure 3 shows the overlapped microstructures given by the lithium and calcium thickeners, where the granular microstructure of the calcium thickener, clearly visualized as spherical particles, appears distributed in the fibrous network provided by the lithium soap.

The AFM technique was also used to analyse the influence of different base oils on the microstructure of four anhydrous calcium soap-based greases. As shown in Figure 2, the C2 microstructure consists of a random granular arrangement of the calcium thickener represented as clumps with different sizes. In the case of grease C3, similar arrangements appear evenly and homogeneously distributed in the matrix of the grease, yielding a more homogeneous and sponge-like structure. These morphologies are associated to vegetable-derived natural base oils which provide more polar interactions with the calcium soap. The differences in both types of samples may be attributed to the soap concentration, presumably lower in sample C2 attending to the NLGI grades (Table 1). On the contrary, completely different microstructures were observed for greases C1 and C4. In both these cases, micrographs display the anhydrous calcium soap thickener in the form of fiber networks, indicating that hydrophobic interactions promoted by non-polar mineral or synthetic oils favour this type of crystallization pattern.

3.4. Frictional working-induced microstructural degradation

Morphological lubricating greases analyses, conducted at completion of tribological testing, are essential sources of information on how wear and friction processes influence grease microstructure as a result of lubrication performance. As previously reported, the structural degradation greatly influences the bulk rheology [7, 18, 20] and the effect of friction on grease structure is referred as rheological wear [33-35]. The influence of frictional tests on the microstructure of three selected lubricating greases was investigated using the AFM technique as can be seen in Figure 5.

AFM micrographs shown in Figure 5 provide a detailed understanding of the changes in microstructure of lithium, methylcellulose and lithium-calcium thickener-phases distributed in the oil matrix occurred during performing tribological tests. A constant rotational speed (400 rpm) of the steel ball on the three inclined steel plates was applied over 10 min using the three greases as lubricant in the contact. AFM technique reveals some interesting features on structural degradation in the three greases. As can be observed in the phase images shown in Figure 5 for sample C5, not dramatic changes in the fibre network arose after performing the constant speed frictional test, resulting thinner and not so agglomerated but more aligned fibres than the same unworked sample (Fig. 5, sample C5a). This means that the frictional test, under these conditions, does not produce any fibre breakdown but mainly the alignment and orientation of fibres in this sample. In this particular grease, designed for operating under extreme conditions of pressure, load and speed, the effect of severe working conditions may be significantly dampened by the high oil viscosity (see Table 1). On the contrary, in sample C6a, less densely arranged lithium soap thickener fibres, and a decrease in diameter of the calcium soap granules may be very well noticed after working (Figure 5). It can also be observed that sample C6a forms an unlike microstructure connecting the lithium thickener in form of longer and orientated fibres to the calcium thickener in form of irregular granules. Regarding sample M1, it is obvious that more drastic microstructural changes appear due to the friction and wear processes. In this case, fibre length was clearly reduced and the fibrous structure appears slightly more agglomerated and randomly orientated (Figure 5, sample M1a). This effect is much more dramatic after performing a rotational speed sweep test between 0.1 and 1000 rpm (see Figure 5 sample M1b). These more severe test conditions amplify the effect of frictional degradation on grease microstructure also in samples C5 and C6. Thus, more pronounced fibre orientation can be detected in sample C5b also slightly reducing fibre length. Similarly, sample C6 showed more reduced size of calcium soap granules, with irregular shape, and not so interconnected in the lithium soap fibrous network after performing a sliding velocity sweep test (see Figure 5 sample C6b). All these morphological changes illustrated in Figure 5 may be directly related to internal frictional and energetic processes as described by Kuhn [34, 35].

4. Conclusions

AFM and SEM techniques were used in this work to produce real space magnified images of greases surface morphology. Lubricating grease microstructure mainly depends on the nature of both the thickener and base oil employed. In the case of anhydrous calcium-base greases used in this study, very different microstructures were encountered depending on the base oil. Thus, the calcium soap thickener appears distributed in the form of fine and slight entangled fibrous arrangement when using non-polar mineral or synthetic base oils whereas a granular structure were found when using vegetable derived oils. In relation to lithium complex soap-based grease, the typical microstructure consisting of a fine dispersion of the crystallized lithium soap in the form of long, twisted and well-entangled fibres were observed. The lithium calcium-complex based grease showed a mixed microstructure where the lithium soap thickener appears distributed in a random manner in form of short and densely arranged fibres while the calcium soap thickener remains dispersed in the grease matrix in form of spherical granules. Regarding the biodegradable biopolymer-based greases, fibrous networks were also detected.

In general, it is possible to conclude that the time-temperature pre-heating protocol plays an important role in AFM analysis. A certain pre-heating treatment on grease samples is generally convenient to improve image resolution. However, an excessive heating results in significant microstructural alterations, particularly agglomeration of thickener structural units.

On the other hand, SEM analysis provided detailed information on the dimensional and spatial distribution of the thickener skeleton, once the base oil was completely removed, normally at lower magnification than AFM. On the contrary, AFM technique allows to determine the arrangement of thickener structure in the presence of the base oil, thus considering the thickener-oil medium interactions, although generally with lower image resolution than SEM. In this sense, it can be stated that SEM and AFM are complementary analysis techniques for lubricating grease microstructural investigations. Despite this fact, similarities between grease microstructures obtained with both techniques were generally found.

Some tribological tests were conducted in order to investigate the influence of high-shear frictional working treatments on lubricating grease. Based on the AFM results obtained, important microstructural changes were observed as a result of the friction and internal wear processes, which depends on both the severity of the frictional working conditions and grease composition. The complex lithium grease structure appeared to be more resistant to relatively gentle working conditions (constant sliding velocity for 10 min) only yielding fibre alignment. On the contrary, the complex lithium-calcium- and especially the functionalized methylcellulose-based thickener structures clearly exhibited a reduction in granule size and fibre length, respectively. More severe frictional working conditions, achieved in a sliding velocity sweep tests, significantly affect the three types of microstructures, resulting in all cases a reduction in the size of the thickener structural units.

5. Acknowledgements

This work is part of two research projects (CTQ2014–56038-C3-1R and TEP-1499) sponsored by MINECO-FEDER and Junta de Andalucía programmes, respectively. The authors gratefully acknowledge the financial support. Authors also acknowledge Castrol (Germany) and Verkol S.A. (Spain) for kindly providing commercial samples.

6. References

1. Gow, G.: Lubricating Grease. In: Mortier, R.M., Fox, M.F., Orszulik, S., (eds.) Chemistry and Technology of Lubricants, 3rd ed., pp. 411-432. Springer Science-Business Media B.V., Heidelberg (2010)
2. National Lubricating Grease Institute: Lubricating Greases Guide. Kansas City, (2006)
3. Franco, J.M., Delgado, M.A., Valencia, C., Sanchez, M.C., Gallegos, C.: Mixing rheometry for studying the manufacture of lubricating greases. Chem. Eng. Sci. 60, 2409–2418 (2005)
4. Mas, R., Magnin, A.: Rheology of colloidal suspensions: Case of lubricating greases, J. Rheol. 38(4), 889-908 (1994)
5. Delgado, M.A., Sanchez, M.C., Valencia, C., Franco, J.M., Gallegos, C.: Relationship among microstructure, rheology and processing of a lithium lubricating grease. Chem. Eng. Res. Des. 83(9), 1085–1092 (2005)
6. Lugt, P.M.: A review on grease lubrication in rolling bearings. Tribol. Trans. 52(4), 470–480 (2009)
7. Couronné, I.D.P.N., Vergne, P., Mazuyer, D., Truong-Dinh, N., Girodin, D.: Effects of grease composition and structure on film thickness in rolling contact. Tribol. Trans. 46(1), 31–36 (2003)
8. Cann, P.M., Grease lubrication of rolling element bearings: role of the grease thickener. Lubr. Sci. 19(3), 183–196 (2007)
9. Morales-Espejel, G.E., Lugt, P.M., Pasaribu, H.R., Cen, H.: Film thickness in grease lubricated slow rotating rolling bearings. Tribol. Int. 74, 7–19 (2014)

10. De Laurentis, N., Kadiric, A., Lugt, P., Cann, P.: The influence of bearing grease composition on friction in rolling/sliding concentrated contacts. Tribol. Int. 94, 624–632 (2016)

11. Kaneta, M., Ogata, T., Takubo, Y., Naka, M.: Effects of a thickener structure on grease elastohydrodynamic lubrication films. Proc. Inst. Mech. Eng., Part J. J. Eng. Tribol. 214(J4), 327–336 (2000)

12. Cyriac, F., Lugt, P.M., Bosman, R., Padberg, C.J., Venner, C.H.: Effect of thickener particle geometry and concentration on the grease EHL film thickness at medium speeds. Tribol. Lett. 61(18), 1-13 (2016)

13. Shuff, P.J., Clarke, L.J.: Imaging of lubricating oil insolubles by Electron Microscopy. Tribol. Int. 24(6), 381-397 (1991)

14. Mansot, J.L., Terech, P., Martin, J.M.: Structural investigation of lubricating greases. Colloids Surf. 39(2), 321–333 (1989)

15. Hurley, S., Cann, P.: Examination of grease structure by SEM and AFM techniques. NLGI Spokesman. 65(5), 17–26 (2001)

16. Rădulescu, I., Rădulescu, A.V., Vasiliu, F.: The Structure of Lubricating Greases by Electron Microscopy. Tribol. Ind. 26(3&4), 58-62 (2004)

17. Baart, P., van der Vorst, B., Lugt, P.M., van Ostayen, R.A.J.: Oil-bleeding model for lubricating grease based on viscous flow through a porous microstructure. Tribol. Trans., 53(3), 340-348 (2010)

18. Sánchez, M.C., Franco, J.M., Valencia, C., Gallegos, C., Urquiola, F., Urchegui, R.: Atomic Force Microscopy and Thermo-Rheological Characterisation of Lubricating Greases. Tribol. Lett. 41(2), 463–70 (2011)

19. Sengupta, P., Noordermeer, J.W.M.: A comparative study of different techniques for microstructural characterization of oil extended thermoplastic elastomer blends. Polym 46, 12298–122305 (2005)

20. Vamos, E., Szamos, J., Bede Gy.: Structural changes in lubricating greases and their mixtures during service. Wear. 25,189-197 (1973)

21. Rizzo, N.W., Irwin, L., Foster, M.D., Funk, M.R.: Extracting, imaging and quantifying soap fibers in grease. NLGI Spokesman. 60(1), 24-25 (1996)

22. Braet, F., Zanger, R., Seynaeve, C., Baekeland, M., Wisse, E.: A comparative atomic force microscopy study on living skin fibroblasts and liver endothelial cells. J. Electron. Microsc. 50, 283–290 (2001)

23. Ushiki T, Nakajima M, Choi M, Cho SJ, Iwata F. Scanning ion conductance microscopy for imaging biological samples in liquid: A comparative study with atomic force microscopy and scanning electron microscopy. Micron. 43(12), 1390–1398 (2012)

24. Katan, A.J., Dekker, C.: High-Speed AFM Reveals the Dynamics of Single Biomolecules at the Nanometer Scale. Cell 147(5), 979–982 (2011)

25. Ando, T., Kodera, N., Takai, E., Maruyama, D., Saito, K., Toda. A.: A high-speed atomic force microscope for studying biological macromolecules. Proc. Natl. Acad. Sci. 98(22), 12468–12472 (2001)

26. Moreno, G., Valencia, C., Paz, M.V., Franco, J.M., Gallegos, C.: Rheology and microstructure of lithium lubricating greases modified with a reactive diisocyanate - terminated polymer: Influence of polymer addition protocol. Chem. Eng. Process. 47(4), 528–538 (2008)

27. Moreno, G., Valencia, C., Franco, J.M., Gallegos, C., Diogo, A., Bordado, J.C.M.: Influence of molecular weight and free NCO content on the rheological

properties of lithium lubricating greases modified with NCO-terminated prepolymers. Eur. Polym. J. 44(7), 2262–2274 (2008)

28. Paszkowski, M., Olsztyńska-Janus, S.: Grease thixotropy: evaluation of grease microstructure change due to shear and relaxation. Ind. Lubr. Tribol. 66(2), 223 – 237 (2014)
29. Gallego, R., Arteaga, J.F., Valencia, C., Diaz, M.J., Franco, J.M.: Gel-Like Dispersions of HMDI-Cross-Linked Lignocellulosic Materials in Castor Oil: Toward Completely Renewable Lubricating Grease Formulations. ACS Sustainable Chem. Eng. 3, 2130−2141 (2015)
30. Gallego, R., Cidade, T., Sánchez, R., Valencia, C., Franco, J.M.: Tribological behaviour of novel chemically modified biopolymer-thickened lubricating greases investigated in a steel–steel rotating ball-on-three plates tribology cell. Tribol. Int. 94, 652–60 (2016)
31. Russell, P., Batchelor, D., Thornton, J.: SEM and AFM: complementary techniques for surface investigations. Application Note AN46, Veeco Instruments Inc., U.S.A. (2004)
32. Paszkowski, M.: Some Aspects of Grease Flow in Lubrication Systems and Friction Nodes. In: Gegner, J. (ed.) Tribology - Fundamentals and Advancements, pp. 77-106. InTech, Croatia (2013)
33. Kuhn, E.: Zur Tribologie der Schmierfette. Expert Verlag, Renningen, Germany (2009), (In German)
34. Kuhn, E.: Analysis of a grease-lubricated contact from an energy point of view. Int. J. Mater. Product. Technol. 38(1), 5-15 (2010)
35. Kuhn, E.: Correlation between system entropy and structural changes in lubricating grease. Lubricants. 3(2), 332-345 (2015)

Tables

Table 1. Composition of lubricating grease samples studied

Lubricating greases	Thickener type	Base oil	Thickener concentration (% wt)	NLGI grade	Dropping point (°C)	Base oil viscosity at 40°C (mm^2/s)
C1	Anhydrous calcium	Mineral oil	-	2	150	68
C2	Anhydrous calcium	Natural ester oil	-	1	150	200
C3	Anhydrous calcium	Castor oil	-	2	150	222
C4	Anhydrous calcium	Synthetic oil	-	2	150	38
C5	Lithium complex	Mineral oil	-	2-3	> 250	1350
C6	Lithium calcium complex	Mineral oil	-	2	260	450
M1	Functionalized methylcellulose	Castor oil	30	2	185	222
M2	Functionalized lignocellulose pulp	Castor oil	7	3-4	160	222

Table 2. Optimum time–temperature combination for AFM sample preparation procedure and operating ranges analyzed

Grease samples	Optimum time-temperature combination		Operating ranges	
	Time (s)	Temperature (°C)	Operating temperature range (°C)	Operating time range (s)
C1	15	100	100-125	15-30
C2	5	150	120-150	5-30
C3	15	150	120-150	5-30
C4	**0**	**25**	**only room temperature**	**-**
C5	15	210	200-225	5-60
C6	30	225	200-240	30-60
M1	30	125	125-150	15-30
M2	5	150	150	5-30

Table 3. Tribological and AFM measurements conditions for lubricating grease samples tested in a tribological contact

Grease samples	**Tribological measurements conditions**			**AFM time–temperature sample preparation procedure applied**	
	normal load (N)	rotational speed, (rpm)	time (min)	temperature (ºC)	time (s)
C5	40	400	12	210	15
	40	0.1-1000	10	210	5
C6	40	400	12	200	15
	40	0.1-1000	10	200	15
M1	40	400	12	125	30
	40	0.1-1000	10	125	30

Figure captions

Fig. 1. Influence of the temperature-time procedure applied on sample preparation for AFM imaging the microstructure of two lubricating greases: C5) a lithium complex grease and C6) a lithium calcium complex grease. (window sizes of 20 µm x 20 µm)

Fig. 2. Comparison between AFM (window sizes of 20 µm x 20 µm and 5 µm x 5 µm) and SEM (15-20kV and 200-5000X magnification) micrographs corresponding to the four anhydrous calcium soap-based greases studied (C1-C4).

Fig. 3. Comparison between AFM (window sizes of 20 µm x 20 µm and 5 µm x 5 µm) and SEM (20kV and 200-13000X magnification) micrographs corresponding to the lithium complex (C5) and lithium calcium complex soap (C6) greases.

Fig. 4. Comparison between AFM (window sizes of 20 µm x 20 µm and 5 µm x 5 µm) and SEM (15kV and 1000-13000X magnification) micrographs corresponding to model biopolymer-based greases: chemically modified methylcellulose- (M1) and lignocellulosic material (M2)-based greases.

Fig. 5. Effect of tribology testing on the morphology of samples C5, C6 and M1. Left side: fresh grease samples; right side: greases submitted to frictional tests, a) 40N at a constant speed of 400 rpm, and b) 40N and rotational speed sweep (0.1-1000 rpm) in a ball-on-plate tribocontact. (window sizes of 20 µm x 20 µm and 5 µm x 5 µm).

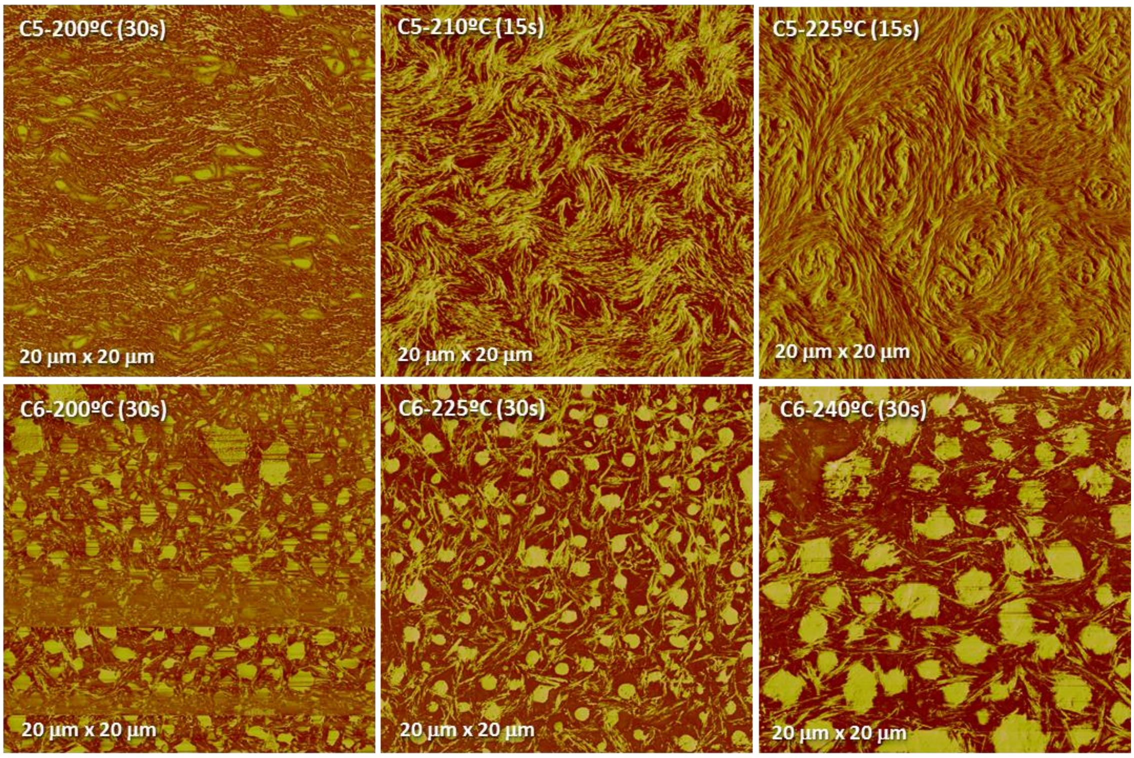
C5-200ºC (30s)
20 μm x 20 μm
C5-210ºC (15s)
20 μm x 20 μm
C5-225ºC (15s)
20 μm x 20 μm
C6-200ºC (30s)
20 μm x 20 μm
C6-225ºC (30s)
20 μm x 20 μm
C6-240ºC (30s)
20 μm x 20 μm

Fig.1.

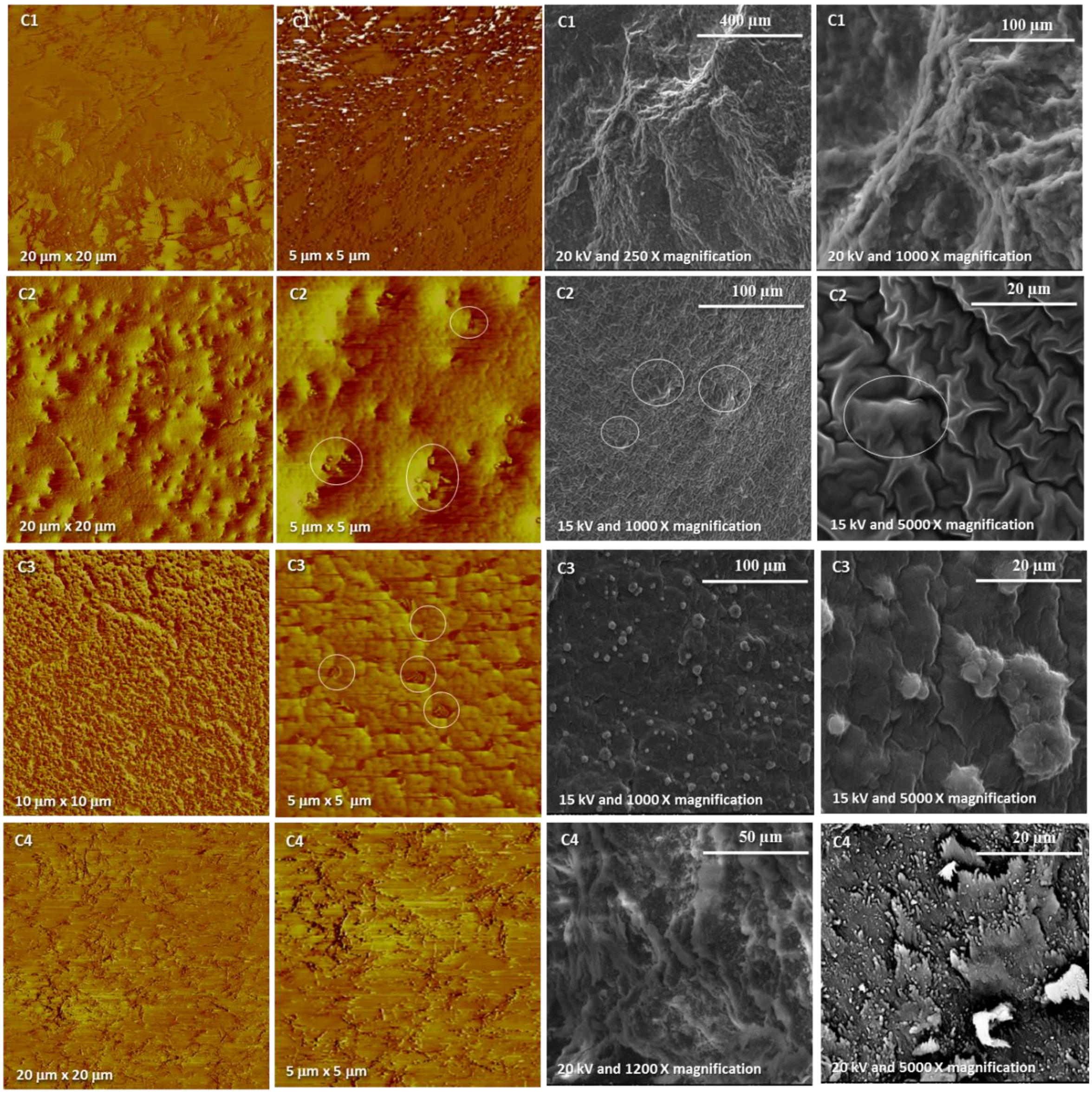
C1
20 µm x 20 µm
C1
5 µm x 5 µm
C1
400 µm
20 kV and 250 X magnification
C1
100 µm
20 kV and 1000 X magnification
C2
20 µm x 20 µm
C2
5 µm x 5 µm
C2
100 µm
15 kV and 1000 X magnification
C2
20 µm
15 kV and 5000 X magnification
C3
10 µm x 10 µm
C3
5 µm x 5 µm
C3
100 µm
15 kV and 1000 X magnification
C3
20 µm
15 kV and 5000 X magnification
C4
20 µm x 20 µm
C4
5 µm x 5 µm
C4
50 µm
20 kV and 1200 X magnification
C4
20 µm
20 kV and 5000 X magnification

Fig.2.

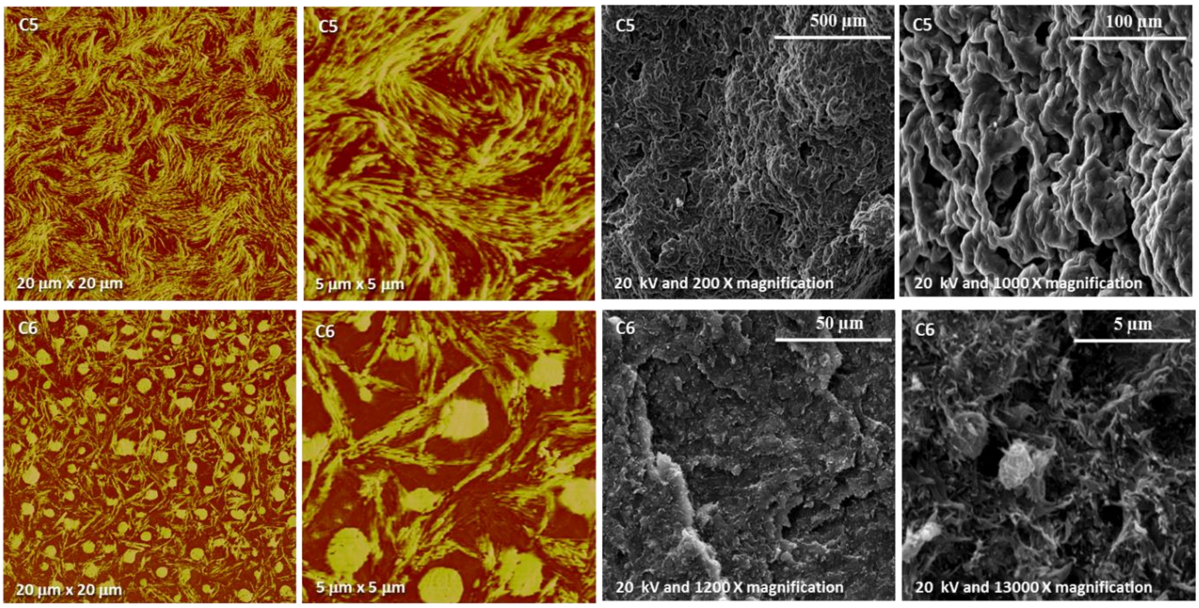
C5
20 µm x 20 µm
C5
5 µm x 5 µm
C5
500 µm
20 kV and 200 X magnification
C5
100 µm
20 kV and 1000 X magnification
C6
20 µm x 20 µm
C6
5 µm x 5 µm
C6
50 µm
20 kV and 1200 X magnification
C6
5 µm
20 kV and 13000 X magnification

Fig.3.

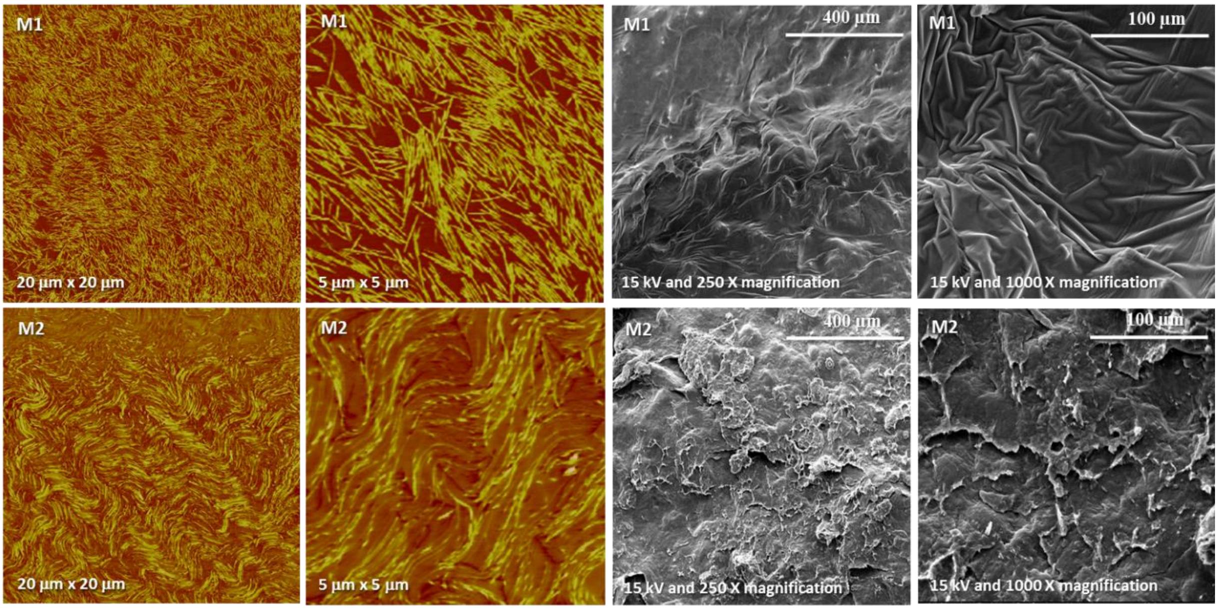
M1
20 µm x 20 µm
M1
5 µm x 5 µm
M1
400 µm
15 kV and 250 X magnification
M1
100 µm
15 kV and 1000 X magnification
M2
20 µm x 20 µm
M2
5 µm x 5 µm
M2
400 µm
15 kV and 250 X magnification
M2
100 µm
15 kV and 1000 X magnification

Fig.4.

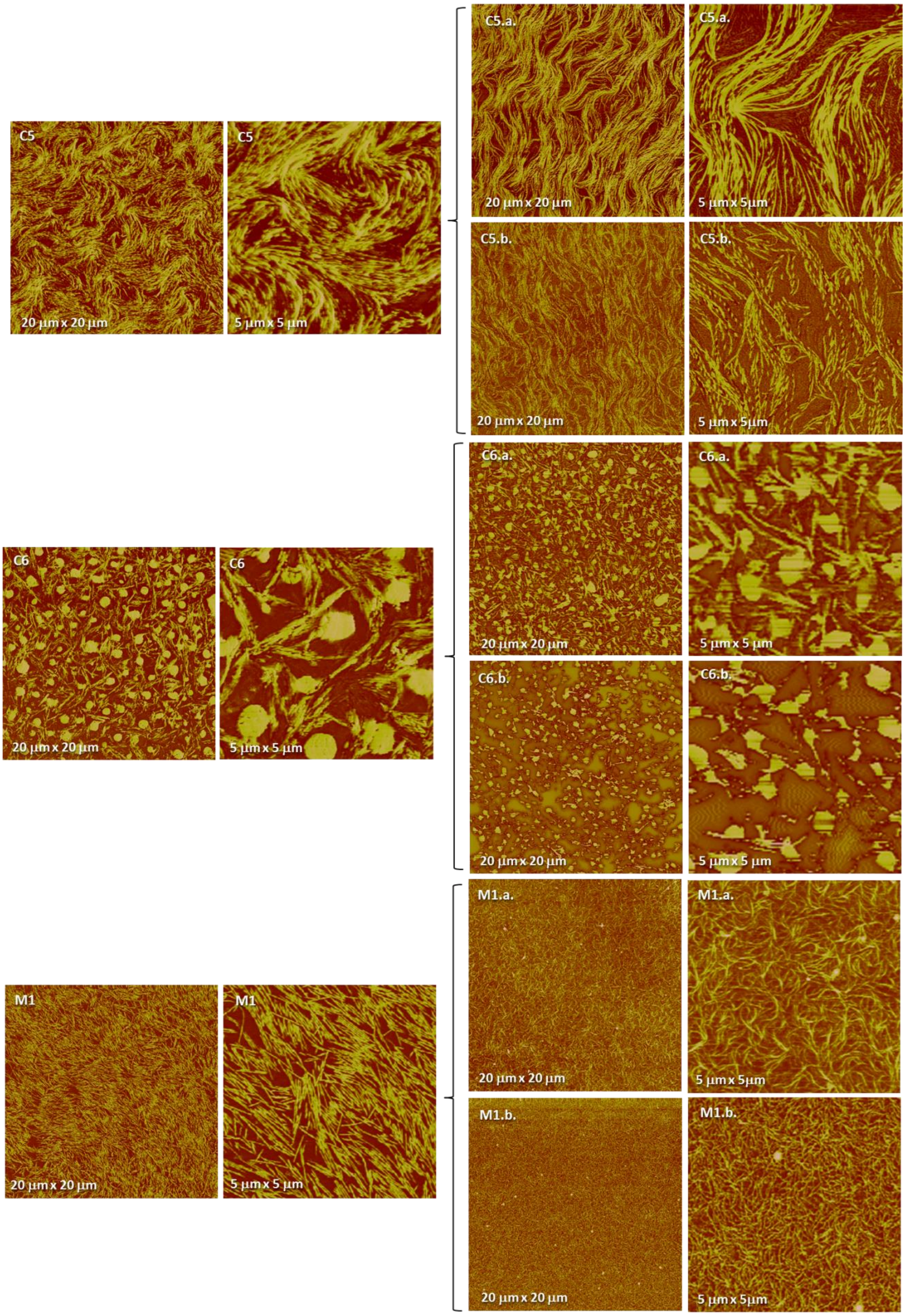
C5
20 µm x 20 µm
C5
5 µm x 5 µm
C5.a.
20 µm x 20 µm
C5.a.
5 µm x 5µm
C5.b.
20 µm x 20 µm
C5.b.
5 µm x 5µm
C6
20 µm x 20 µm
C6
5 µm x 5 µm
C6.a.
20 µm x 20 µm
C6.a.
5 µm x 5 µm
C6.b.
20 µm x 20 µm
C6.b.
5 µm x 5 µm
M1
20 µm x 20 µm
M1
5 µm x 5 µm
M1.a.
20 µm x 20 µm
M1.a.
5 µm x 5µm
M1.b.
20 µm x 20 µm
M1.b.
5 µm x 5µm

Fig.5.

AFM and SEM assessment of lubricating grease microstructures: influence of sample preparation protocol, frictional working conditions and composition

C. Roman, C. Valencia, J. M. Franco✉

Chemical Process and Product Technology Research Center (Pro^{2}TecS).

Dept Ingeniería Química Campus de 'El Carmen', Universidad de Huelva. 21071 Huelva. Spain.

✉ Author to whom correspondence should be addressed:

E-mail address: franco@uhu.es.

Tel.: +34959219995

Fax: +34959219983

Abstract

The microstructure of lubricating greases greatly conditions their in-service performance. In that sense, optimal testing protocols are required in order to accomplish their correct morphological characterization. This study explores and compares the suitability of Atomic Force Microscopy (AFM) and Scanning Electron Microscopy (SEM) techniques for imaging six different commercial metallic soap-based greases and two novel biopolymer-based formulations. Pros and cons of both techniques as well as the effect of sample preparation protocol were analyzed. The results revealed a wide variety of morphological characteristics depending on composition. Thus, the four anhydrous calcium-based greases demonstrated two clearly distinct microstructures (fibrous and granular) determined by the type of base oil employed. With regard to the lithium complex greases, the typically reported microstructure characterized by well-defined entangled and fibrous network was observed in both AFM and SEM techniques. As for the two biopolymer-based greases, fiber networks were also encountered. Besides this, selected greases were subjected to different tribological tests, and the effect of high-shear frictional working treatments on their microstructure was also analyzed. As a result of the friction and internal wear, the AFM results evidenced microstructural changes which depended on grease composition. Overall, the combined use of AFM and SEM techniques was demonstrated to be a powerful approach to microstructurally characterize lubricating greases.

Keywords: AFM; SEM; lubricating grease; microstructure; friction

1. Introduction

Nowadays, lubricating greases are of utmost importance for both a wide variety of industrial applications and everyday lubrication challenges as they are designed to maximize efficiency and prolong the useful service life of all moving equipment [1]. In general, the design and development of lubricants require ample experience and knowledge to obtain an appropriate behavior for specific applications. In the particular case of lubricating greases, further adequate microstructure and related physical properties must be reached from an appropriate sequence selection of both grease ingredients and manufacturing process [2, 3].

Lubricating greases are essentially highly-structured two-phase colloidal suspensions consisting of a thickening agent, usually a metal soap, such as lithium, sodium and calcium salts of long chain fatty acids, dispersed in a lubricating liquid such as mineral, synthetic or vegetable-derived oils. The thickener forms a three-dimensional gelling network which traps the oil and confers the appropriate rheological and tribological behavior to the grease [4, 5]. These particular rheological characteristics imparted by the thickener make lubricating greases more convenient in some applications where lubricating oils do not work properly, like rolling bearings. Actually, factors like decreasing leakage and frequency of lubrication in hard-to-reach contacts, fluctuations with temperature, loads, vibrations, etc. can be minimized when using greases [6]. Apart from the main lubrication role, which is mainly performed by the lubricating oil, the rest of differential and characteristic performance properties of lubricating greases are due to the microstructure. Several authors have highlighted the role of the thickener in film thickness [7-10], some of them emphasizing the thickener microstructure [11]. Recently, Cyriac et al. [12] pointed out in a very elucidating work the importance of grease microstructure on the lubrication film thickness, demonstrating that the smaller thickener structural units, the thicker films were obtained. Hence, acquiring new knowledge and understanding on how the microstructure of grease thickener can provide functional properties for both, good lubrication performance and lifetime is essential.

Microscopy methods like atomic force microscopy (AFM), scanning electron microscopy (SEM) or transmission electron microscopy (TEM), reveals micro- and nanoscale structural details, and therefore are powerful and effective tools for visualising the lubricating grease morphology [13-18]. However, in spite of the continual development and great diversity of microscopy techniques, microstructure determination of lubricating greases remains a current challenge. This is because most electron microscopy methods are based on observations of thin sections or surfaces that show a cross-section of the structure. Besides that, some surface topographies of soft specimens could be affected by the sample preparation/treatment method [19].

Despite the fact that there is a rather extensive literature describing the use of TEM and SEM techniques to investigate the grease microstructure [13, 14, 16, 20], the two techniques present some drawbacks. Both of them are vacuum based and, therefore the oil component must be removed or its volatility reduced before analysis, for instance by freezing the sample. The most common criticism associated to SEM and TEM analysis is that these techniques can alter the original grease microstructure [14, 16, 21] as a result of modifying the thickener-oil interaction balance. For instance, much more agglomerated structural units have been observed using the SEM technique in washed samples than those observed in non-washed samples using the AFM technique [12].

Taking into account that greases may contain large amount of lubrication oil, one of the main goals in this study was to establish a reliable method to observe the thickener microstructure of different lubricating greases by preserving the integrity of the samples as much as possible. In particular, since the AFM can work in various environments (vacuum, air and liquid), many researchers have been interested in imaging soft or biological samples [22, 23]. Furthermore, recent advances in AFM have enabled high-speed imaging of soft samples allowing the direct visualization of biomolecules [24, 25]. So far, some specific observations of grease microstructures by means of atomic force microscopy have been previously reported [12, 15, 18, 26-29]. However, it still remains difficult to image the nanoscale topography of lubricating grease samples by AFM, because some artifacts can arise due to non-desired interactions between the tip and the sample as a consequence of several factors such as tip geometry, lateral forces or grease textural and rheological properties. For instance, soft greases having low consistency can induce the sticking of the tip to the sample and consequently, the AFM image on the specimen microstructure can show artefacts or cannot be obtained. In this sense, Hurley and Cann [11] were not able to obtain good observations in non-washed samples using the contact mode. Some of these problems can be avoided by heating the grease sample below the dropping point and then cooling down to obtain smooth enough films [18, 26, 27]. However, this pre-heating protocol must be also optimized to avoid any change in the thickener-oil interaction balance. In spite of the mentioned limitations, this technique provides great advantages, as the microstructure analysis can be performed under atmospheric pressure and enables to visualize surface microstructure in almost non-perturbed grease samples.

Taking into account these considerations, this work aims to investigate the topography (surface features) and morphology (overall shape) of different lubricating greases, including several commercial samples with different composition and some novel biopolymers-based grease formulations, by means of SEM and AFM techniques and compare the information that can be derived from both techniques. The pre-heating protocol to obtain accurate AFM observations on non-washed samples was optimized. In addition, the effect of high-shear working treatments on lubricating grease microstructure in some tribological tests was also explored on selected samples.

2. Experimental

2.1. Materials

Eight lubricating grease samples differing on their composition were analysed from a microstructural point of view. Samples C1-C6 were commercially available calcium and lithium soap-based greases whereas biopolymer-based model samples M1 and M2 were manufactured in the laboratory as described elsewhere [29, 30]. Compositional details of the different lubricating greases analysed in this study as well as basic properties are listed in Table 1. The selection of grease samples was done according to the different compositional variables aimed to be studied, i.e. type of thickener and type and viscosity of base oil.

2.2. AFM observations

Morphological observations of grease samples were investigated using a multimode AFM connected to a Nanoscope IV scanning probe microscope controller (Digital Instruments, Veeco Metrology Group Inc., Santa Barbara, CA) using the tapping mode with phase detection imaging at room temperature. Tapping mode amplitude modulation microscopy is an adequate approach for imaging soft materials such as lubricating greases because it involves the repeated oscillation of the cantilever at or slightly below its resonant frequency. The amplitude of oscillation typically ranges from

20 nm to 100 nm. The tip lightly interacts with the sample surface during scanning providing high resolution images with minimum sample damage. Silicon Nanosensors™ PPP-NCH AFM probes for tapping mode with a force constant of 42 N/m and resonance frequency of 330 kHz were used. Scan speed was set at 1 Hz and scan windows were taken from 5 to 20 μm.

In order to obtain good imaging quality the specimens for AFM examination require an appropriate preliminary preparation. Grease sample preparation for accurate observations is one of the most challenging and essential steps in AFM microstructural analysis because of the grease low consistency. A pre-heating treatment at a temperature below the dropping point of the lubricating grease was applied in order to form a smooth surface which yields a good resolution. A MR Hei Standard hotplate from Heidolph was used for heating grease samples. Different time-temperature combinations comprised between 100 ºC and 240 ºC for 5-30 s were tested depending on the sample. The optimized time-temperature procedures established for each sample are included in Table 2. Afterwards, samples were cooled down to room temperature for some minutes before placing them in the AFM holder and starting the scan sequence. In the particular case of sample C4, accurate observations were only feasible without heating the sample.

2.3. SEM observations

The morphological analysis of the lubricating greases by means of scanning electron microscopy (SEM) was performed in a JEOL microscope (Japan), model JSM-5410, operating at 15 and 20 kV accelerating voltages. This scanning electron microscope covers the practical magnification range from 200X to 13 000X.

Since SEM requires a hard vacuum in the sample chamber, the extraction of oil was absolutely necessary to image the sample morphology. In the process of SEM analysis, preliminary treatment of the lubricating grease is one of the most time consuming steps. The goal of extraction process is effective isolation of the thickener agent from the matrix by use of a non-polar organic solvent with minimal effect on specimens. Hence, oil was extracted by immersing the sample for one week in n-hexane. The solvent was carefully replaced 3 - 4 times per day, until oil extraction was completed. Afterwards, the samples were stored and dried at room temperature for a period of some days until ready for use. Moreover, as conventionally done, in order to prevent charging of the surface, reduce thermal damage and improve the secondary electron signal required for topographic examination in the SEM, the samples were coated with a thin layer of gold by means of a sputter coater HHV Scancoat Six SEM.

2.4. Tribological measurements

Three selected greases (C5, C6 and M1) were used as lubricants in a tribological contact in order to evaluate the effect of a severe working treatment on grease microstructure. Samples were placed in a tribological cell coupled with a controlled-stress rheometer, Physica MCR-501 (Anton Paar, Austria), as described elsewhere [30]. At least three replicates of each test were performed at room temperature on fresh samples and resulting worked grease samples were analyzed by AFM. Tribological test conditions are collected in Table 3.

3. Results and Discussion

3.1. Influence of sample preparation protocol

The influence of the pre-heating treatment on AFM imaging lubricating grease microstructures was analysed on samples C5, a lithium complex-based grease, and C6, a lithium-calcium complex grease. Figure 1 shows selected AFM micrographs of these samples obtained after applying different pre-heating temperatures and times. As can be observed, there are significant microstructural similarities between the same samples as long as the applied temperature was well below the dropping point of the grease and the heating time was not longer than typically 15-30 s. However, the time-temperature combination which produces significant changes in the microstructure depends on grease consistency and thickener type.

It can also be noticed that the typical entangled fibrous microstructure is apparent in sample C5 when heating at 200 ºC for 30 s, where long and twisted individual fibres can be detected. AFM phase micrographs still display the lithium soap thickener in the form of highly entangled but slightly more agglomerated fibre network when pre-heating the sample at 210 ºC for 15 s. However, much more agglomerated fibres and compact structure can be visualized at 225 ºC.

Regarding sample C6, the lithium-calcium complex thickener forms a connecting fibrous-granular microstructure, where the calcium soap appears dispersed and homogeneously distributed in the form of granules of around 0.5 μm in a fibrous network, which can be roughly observed by pre-heating the sample at 200 ºC. The same microstructure can be visualized with better resolution by pre-heating the sample at 225 ºC. However, after heating at 240 ºC, rather close to the dropping point (see Table 1), a significant change in the microstructure can be clearly detected. The lithium soap thickener appears like shorter and less intricate fibres network while the calcium soap thickener remains dispersed in the grease matrix in form of larger spherical granules, with sizes of around 2-4 μm. This increase in diameter of the calcium granules for sample C4 could be attributed to a partial melting of the calcium thickener and further re-crystallization. Furthermore, the base oil could evaporate at the surface producing the agglomeration of thickener particles. These results strongly suggest that it is essential to determine the right time-temperature procedure before AFM imaging a specific lubricating grease. In the next sections, AFM images obtained after optimizing the pre-heating protocol are shown. The optimization of this pre-heating treatment dealt with the application of different time-temperature combinations, in the ranges shown in Table 2 for each specific grease, and the evaluation of the resulting microstructure. Typically, the higher temperature and/or heating time, the higher resolution was found. The optimum time-temperature combinations were considered those providing the higher image resolution without inducing any significant microstructural change compared to the non-heated or just slightly heated microstructure.

3.2. Comparison between AFM and SEM imaging of lubricating grease microstructures

Although grease sample preparation for SEM and AFM imaging is really different, actually they are complementary techniques. Thus, the AFM is adequate technique at measuring surface height of the almost unperturbed sample, often at extremely high resolution, while the SEM provides elemental analysis of the surface by detecting sharp changes in height or slope of the thickener skeleton. Furthermore, one technique often compensates for the imaging artefact of the other [31].

AFM and SEM techniques were used to examine the eight different lubricating grease samples studied and actually similar microstructures were obtained. In general, two main distinct types of thickener structure (fibrous and/or granular) were possible to observe in both AFM and SEM micrographs. The AFM images reported in this section were performed by using the tapping mode in phase imaging once considered the optimum time-temperature sample preparation procedure which was previously determined (see Table 2).

Figures 2-4 show a comparison between the phase images taken by AFM and SEM micrographs for the different lubricating greases studied. The two techniques present different principles of operation and therefore the micrographs are presented in different arrangements and window sizes. However, it is evident that all microstructures determined by AFM are quite similar to those obtained by SEM analysis, which demonstrates that oil extraction does not exert a great influence in the thickener arrangement, at least from a qualitative point of view. Thus, the main difference observed between the two sets of images is that SEM microstructures seem to appear more agglomerated and collapsed as a consequence of oil removing. In a few cases, the structural units are not easily detectable as a result of this collapse (see for instance Figure 2, sample C4, and Figure 4, sample M2). Figure 2 shows different anhydrous calcium soap microstructures formed in different oil media. Taking into account that all samples are anhydrous calcium-based greases, completely different microstructures of the soap thickener can be observed in both AFM and SEM analysis. Thus, the microstructure of samples C1 and C4 consist of fine, small and slightly entangled and twisted fibres as previously described [13,32], whereas a granular and/or sponge-like thickener microstructure was detected in both AFM and SEM micrographs for samples C2 and C3, when the thickener was dispersed in vegetable-derived oils. However, a certain degree of crosslinked structures can be distinguished for sample C2 in the SEM image taken at the highest magnification (Figure 2). On the other hand, a well-formed, twisted and tangled fibrous network with thicker fibres but more agglomerated can be detected by SEM operating with 20 kV accelerating voltage and 1000X-1200X magnification for samples C1 and C4.

The typical twisted and tangled fibrous arrangements of lithium greases were observed in sample C5 (Figure 3) using both AFM and SEM techniques. Due to the interactions between these colloidal particles and oil phase, these fibres have the ability to arrange themselves into a specific fibrous microstructure. This characteristic lithium soap arrangement is more evident in AFM images where the oil is present.

Concerning sample C6, the above discussed characteristic mixed structure, where the lithium soap thickener appears distributed in a random manner in form of short and dense fibres and the calcium soap thickener remains dispersed in the grease matrix in form of spherical granules, was evidenced. Inspection of AFM images in Figure 3 reveals a quite complex phase behaviour of the two metallic soaps with the capacity to perfectly immobilise the base oil. This particular microstructure is the most affected by oil removing. However, still using the SEM technique it was possible to observe the same structural network of granules dispersed in a fibrous structure (Figure 3).

Finally, Figure 4 shows selected AFM and SEM images of the two model biopolymer-based greases used in this study. In the case of both samples, M1 and M2, it was possible to observe a quite dense and tangled fibrous network which very much resembles a lithium soap microstructure. Much finer and shorter fibres were observed in the microstructure provided by the chemically modified methylcellulose (M1) using the AFM technique. The fibres structure is also easily detectable in SEM images for sample M1, although at different scale. However, the long and twisted fibres observed with AFM in the lignocellulosic material-based grease (sample M2) were not really well appreciated by SEM analysis, where only at 1000X magnification a fibrous structure can be guessed.

3.3. Influence of compositional variables

As can be deduced from the microscopy observations previously discussed, the morphology of grease structure greatly depends on the composition, both type of thickener and base oil. The typical morphologies given by the most common thickener agents have been previously reported [4,13-15,18]. However, the influence of either the base oil or the interaction between the base oil and the thickener has not still been investigated in detail. Most widely used thickening agents in grease formulations are fatty acid soaps of lithium and calcium. The AFM and SEM images of three different calcium (C1), lithium (C5), and lithium-calcium (C6) thickening agents dispersed in a mineral oil are compared (see Figures 1 and 2). Presuming similar hydrophobic interactions between the mineral base oil and the fatty acid soaps, the different morphologies are essentially due to the typical crystallization patterns of each fatty acid soap. Microstructures of anhydrous and lithium complex soaps encountered in this study are in agreement with those previously reported in the literature taken by SEM and TEM analysis [13-16]. Relatively short, thin and not especially agglomerated fibres can be observed by means of AFM analysis in the case of grease C1. This sample was difficult to image after pre-heating by means of AFM due to an excessive softening of the sample. This behaviour is particularly associated with a low viscosity of the base oil (see Table 1). Hence, greases containing a low-viscosity base oil or high content of oil, i.e. soft greases, may give poor images and some artefacts during scanning due to contamination of the AFM-tip by the oil. The entangled fibrous structure of the anhydrous calcium-based grease examined (C1) can be also observed in Figure 2 by SEM. With regard to the lithium complex grease (sample C5), the typical fibrous and entangled microstructure was observed in both AFM and SEM techniques (see Figure 3). Finally, in the case of sample C6, as previously discussed, Figure 3 shows the overlapped microstructures given by the lithium and calcium thickeners, where the granular microstructure of the calcium thickener, clearly visualized as spherical particles, appears distributed in the fibrous network provided by the lithium soap.

The AFM technique was also used to analyse the influence of different base oils on the microstructure of four anhydrous calcium soap-based greases. As shown in Figure 2, the C2 microstructure consists of a random granular arrangement of the calcium thickener represented as clumps with different sizes. In the case of grease C3, similar arrangements appear evenly and homogeneously distributed in the matrix of the grease, yielding a more homogeneous and sponge-like structure. These morphologies are associated to vegetable-derived natural base oils which provide more polar interactions with the calcium soap. The differences in both types of samples may be attributed to the soap concentration, presumably lower in sample C2 attending to the NLGI grades (Table 1). On the contrary, completely different microstructures were observed for greases C1 and C4. In both these cases, micrographs display the anhydrous calcium soap thickener in the form of fiber networks, indicating that hydrophobic interactions promoted by non-polar mineral or synthetic oils favour this type of crystallization pattern.

3.4. Frictional working-induced microstructural degradation

Morphological lubricating greases analyses, conducted at completion of tribological testing, are essential sources of information on how wear and friction processes influence grease microstructure as a result of lubrication performance. As previously reported, the structural degradation greatly influences the bulk rheology [7, 18, 20] and the effect of friction on grease structure is referred as rheological wear [33-35]. The influence of frictional tests on the microstructure of three selected lubricating greases was investigated using the AFM technique as can be seen in Figure 5.

AFM micrographs shown in Figure 5 provide a detailed understanding of the changes in microstructure of lithium, methylcellulose and lithium-calcium thickener-phases distributed in the oil matrix occurred during performing tribological tests. A constant rotational speed (400 rpm) of the steel ball on the three inclined steel plates was applied over 10 min using the three greases as lubricant in the contact. AFM technique reveals some interesting features on structural degradation in the three greases. As can be observed in the phase images shown in Figure 5 for sample C5, not dramatic changes in the fibre network arose after performing the constant speed frictional test, resulting thinner and not so agglomerated but more aligned fibres than the same unworked sample (Fig. 5, sample C5a). This means that the frictional test, under these conditions, does not produce any fibre breakdown but mainly the alignment and orientation of fibres in this sample. In this particular grease, designed for operating under extreme conditions of pressure, load and speed, the effect of severe working conditions may be significantly dampened by the high oil viscosity (see Table 1). On the contrary, in sample C6a, less densely arranged lithium soap thickener fibres, and a decrease in diameter of the calcium soap granules may be very well noticed after working (Figure 5). It can also be observed that sample C6a forms an unlike microstructure connecting the lithium thickener in form of longer and orientated fibres to the calcium thickener in form of irregular granules. Regarding sample M1, it is obvious that more drastic microstructural changes appear due to the friction and wear processes. In this case, fibre length was clearly reduced and the fibrous structure appears slightly more agglomerated and randomly orientated (Figure 5, sample M1a). This effect is much more dramatic after performing a rotational speed sweep test between 0.1 and 1000 rpm (see Figure 5 sample M1b). These more severe test conditions amplify the effect of frictional degradation on grease microstructure also in samples C5 and C6. Thus, more pronounced fibre orientation can be detected in sample C5b also slightly reducing fibre length. Similarly, sample C6 showed more reduced size of calcium soap granules, with irregular shape, and not so interconnected in the lithium soap fibrous network after performing a sliding velocity sweep test (see Figure 5 sample C6b). All these morphological changes illustrated in Figure 5 may be directly related to internal frictional and energetic processes as described by Kuhn [34, 35].

4. Conclusions

AFM and SEM techniques were used in this work to produce real space magnified images of greases surface morphology. Lubricating grease microstructure mainly depends on the nature of both the thickener and base oil employed. In the case of anhydrous calcium-base greases used in this study, very different microstructures were encountered depending on the base oil. Thus, the calcium soap thickener appears distributed in the form of fine and slight entangled fibrous arrangement when using non-polar mineral or synthetic base oils whereas a granular structure were found when using vegetable derived oils. In relation to lithium complex soap-based grease, the typical microstructure consisting of a fine dispersion of the crystallized lithium soap in the form of long, twisted and well-entangled fibres were observed. The lithium calcium-complex based grease showed a mixed microstructure where the lithium soap thickener appears distributed in a random manner in form of short and densely arranged fibres while the calcium soap thickener remains dispersed in the grease matrix in form of spherical granules. Regarding the biodegradable biopolymer-based greases, fibrous networks were also detected.

In general, it is possible to conclude that the time-temperature pre-heating protocol plays an important role in AFM analysis. A certain pre-heating treatment on grease samples is generally convenient to improve image resolution. However, an excessive heating results in significant microstructural alterations, particularly agglomeration of thickener structural units.

On the other hand, SEM analysis provided detailed information on the dimensional and spatial distribution of the thickener skeleton, once the base oil was completely removed, normally at lower magnification than AFM. On the contrary, AFM technique allows to determine the arrangement of thickener structure in the presence of the base oil, thus considering the thickener-oil medium interactions, although generally with lower image resolution than SEM. In this sense, it can be stated that SEM and AFM are complementary analysis techniques for lubricating grease microstructural investigations. Despite this fact, similarities between grease microstructures obtained with both techniques were generally found.

Some tribological tests were conducted in order to investigate the influence of high-shear frictional working treatments on lubricating grease. Based on the AFM results obtained, important microstructural changes were observed as a result of the friction and internal wear processes, which depends on both the severity of the frictional working conditions and grease composition. The complex lithium grease structure appeared to be more resistant to relatively gentle working conditions (constant sliding velocity for 10 min) only yielding fibre alignment. On the contrary, the complex lithium-calcium- and especially the functionalized methylcellulose-based thickener structures clearly exhibited a reduction in granule size and fibre length, respectively. More severe frictional working conditions, achieved in a sliding velocity sweep tests, significantly affect the three types of microstructures, resulting in all cases a reduction in the size of the thickener structural units.

5. Acknowledgements

This work is part of two research projects (CTQ2014–56038-C3-1R and TEP-1499) sponsored by MINECO-FEDER and Junta de Andalucía programmes, respectively. The authors gratefully acknowledge the financial support. Authors also acknowledge Castrol (Germany) and Verkol S.A. (Spain) for kindly providing commercial samples.

6. References

1. Gow, G.: Lubricating Grease. In: Mortier, R.M., Fox, M.F., Orszulik, S., (eds.) Chemistry and Technology of Lubricants, 3rd ed., pp. 411-432. Springer Science-Business Media B.V., Heidelberg (2010)
2. National Lubricating Grease Institute: Lubricating Greases Guide. Kansas City, (2006)
3. Franco, J.M., Delgado, M.A., Valencia, C., Sanchez, M.C., Gallegos, C.: Mixing rheometry for studying the manufacture of lubricating greases. Chem. Eng. Sci. 60, 2409–2418 (2005)
4. Mas, R., Magnin, A.: Rheology of colloidal suspensions: Case of lubricating greases, J. Rheol. 38(4), 889-908 (1994)
5. Delgado, M.A., Sanchez, M.C., Valencia, C., Franco, J.M., Gallegos, C.: Relationship among microstructure, rheology and processing of a lithium lubricating grease. Chem. Eng. Res. Des. 83(9), 1085–1092 (2005)
6. Lugt, P.M.: A review on grease lubrication in rolling bearings. Tribol. Trans. 52(4), 470–480 (2009)
7. Couronné, I.D.P.N., Vergne, P., Mazuyer, D., Truong-Dinh, N., Girodin, D.: Effects of grease composition and structure on film thickness in rolling contact. Tribol. Trans. 46(1), 31–36 (2003)
8. Cann, P.M., Grease lubrication of rolling element bearings: role of the grease thickener. Lubr. Sci. 19(3), 183–196 (2007)
9. Morales-Espejel, G.E., Lugt, P.M., Pasaribu, H.R., Cen, H.: Film thickness in grease lubricated slow rotating rolling bearings. Tribol. Int. 74, 7–19 (2014)

10. De Laurentis, N., Kadiric, A., Lugt, P., Cann, P.: The influence of bearing grease composition on friction in rolling/sliding concentrated contacts. Tribol. Int. 94, 624–632 (2016)
11. Kaneta, M., Ogata, T., Takubo, Y., Naka, M.: Effects of a thickener structure on grease elastohydrodynamic lubrication films. Proc. Inst. Mech. Eng., Part J. J. Eng. Tribol. 214(J4), 327–336 (2000)
12. Cyriac, F., Lugt, P.M., Bosman, R., Padberg, C.J., Venner, C.H.: Effect of thickener particle geometry and concentration on the grease EHL film thickness at medium speeds. Tribol. Lett. 61(18), 1-13 (2016)
13. Shuff, P.J., Clarke, L.J.: Imaging of lubricating oil insolubles by Electron Microscopy. Tribol. Int. 24(6), 381-397 (1991)
14. Mansot, J.L., Terech, P., Martin, J.M.: Structural investigation of lubricating greases. Colloids Surf. 39(2), 321–333 (1989)
15. Hurley, S., Cann, P.: Examination of grease structure by SEM and AFM techniques. NLGI Spokesman. 65(5), 17–26 (2001)
16. Rădulescu, I., Rădulescu, A.V., Vasiliu, F.: The Structure of Lubricating Greases by Electron Microscopy. Tribol. Ind. 26(3&4), 58-62 (2004)
17. Baart, P., van der Vorst, B., Lugt, P.M., van Ostayen, R.A.J.: Oil-bleeding model for lubricating grease based on viscous flow through a porous microstructure. Tribol. Trans., 53(3), 340-348 (2010)
18. Sánchez, M.C., Franco, J.M., Valencia, C., Gallegos, C., Urquiola, F., Urchegui, R.: Atomic Force Microscopy and Thermo-Rheological Characterisation of Lubricating Greases. Tribol. Lett. 41(2), 463–70 (2011)

19. Sengupta, P., Noordermeer, J.W.M.: A comparative study of different techniques for microstructural characterization of oil extended thermoplastic elastomer blends. Polym 46, 12298–122305 (2005)

20. Vamos, E., Szamos, J., Bede Gy.: Structural changes in lubricating greases and their mixtures during service. Wear. 25,189-197 (1973)

21. Rizzo, N.W., Irwin, L., Foster, M.D., Funk, M.R.: Extracting, imaging and quantifying soap fibers in grease. NLGI Spokesman. 60(1), 24-25 (1996)

22. Braet, F., Zanger, R., Seynaeve, C., Baekeland, M., Wisse, E.: A comparative atomic force microscopy study on living skin fibroblasts and liver endothelial cells. J. Electron. Microsc. 50, 283–290 (2001)

23. Ushiki T, Nakajima M, Choi M, Cho SJ, Iwata F. Scanning ion conductance microscopy for imaging biological samples in liquid: A comparative study with atomic force microscopy and scanning electron microscopy. Micron. 43(12), 1390–1398 (2012)

24. Katan, A.J., Dekker, C.: High-Speed AFM Reveals the Dynamics of Single Biomolecules at the Nanometer Scale. Cell 147(5), 979–982 (2011)

25. Ando, T., Kodera, N., Takai, E., Maruyama, D., Saito, K., Toda. A.: A high-speed atomic force microscope for studying biological macromolecules. Proc. Natl. Acad. Sci. 98(22), 12468–12472 (2001)

26. Moreno, G., Valencia, C., Paz, M.V., Franco, J.M., Gallegos, C.: Rheology and microstructure of lithium lubricating greases modified with a reactive diisocyanate - terminated polymer: Influence of polymer addition protocol. Chem. Eng. Process. 47(4), 528–538 (2008)

27. Moreno, G., Valencia, C., Franco, J.M., Gallegos, C., Diogo, A., Bordado, J.C.M.: Influence of molecular weight and free NCO content on the rheological

properties of lithium lubricating greases modified with NCO-terminated prepolymers. Eur. Polym. J. 44(7), 2262–2274 (2008)

28. Paszkowski, M., Olsztyńska-Janus, S.: Grease thixotropy: evaluation of grease microstructure change due to shear and relaxation. Ind. Lubr. Tribol. 66(2), 223 – 237 (2014)
29. Gallego, R., Arteaga, J.F., Valencia, C., Diaz, M.J., Franco, J.M.: Gel-Like Dispersions of HMDI-Cross-Linked Lignocellulosic Materials in Castor Oil: Toward Completely Renewable Lubricating Grease Formulations. ACS Sustainable Chem. Eng. 3, 2130−2141 (2015)
30. Gallego, R., Cidade, T., Sánchez, R., Valencia, C., Franco, J.M.: Tribological behaviour of novel chemically modified biopolymer-thickened lubricating greases investigated in a steel–steel rotating ball-on-three plates tribology cell. Tribol. Int. 94, 652–60 (2016)
31. Russell, P., Batchelor, D., Thornton, J.: SEM and AFM: complementary techniques for surface investigations. Application Note AN46, Veeco Instruments Inc., U.S.A. (2004)
32. Paszkowski, M.: Some Aspects of Grease Flow in Lubrication Systems and Friction Nodes. In: Gegner, J. (ed.) Tribology - Fundamentals and Advancements, pp. 77-106. InTech, Croatia (2013)
33. Kuhn, E.: Zur Tribologie der Schmierfette. Expert Verlag, Renningen, Germany (2009), (In German)
34. Kuhn, E.: Analysis of a grease-lubricated contact from an energy point of view. Int. J. Mater. Product. Technol. 38(1), 5-15 (2010)
35. Kuhn, E.: Correlation between system entropy and structural changes in lubricating grease. Lubricants. 3(2), 332-345 (2015)

Tables

Table 1. Composition of lubricating grease samples studied

Lubricating greases	Thickener type	Base oil	Thickener concentration (% wt)	NLGI grade	Dropping point (ºC)	Base oil viscosity at 40ºC (mm^2/s)
C1	Anhydrous calcium	Mineral oil	-	2	150	68
C2	Anhydrous calcium	Natural ester oil	-	1	150	200
C3	Anhydrous calcium	Castor oil	-	2	150	222
C4	Anhydrous calcium	Synthetic oil	-	2	150	38
C5	Lithium complex	Mineral oil	-	2-3	> 250	1350
C6	Lithium calcium complex	Mineral oil	-	2	260	450
M1	Functionalized methylcellulose	Castor oil	30	2	185	222
M2	Functionalized lignocellulose pulp	Castor oil	7	3-4	160	222

Table 2. Optimum time–temperature combination for AFM sample preparation procedure and operating ranges analyzed

Grease samples	Optimum time-temperature combination		Operating ranges	
	Time (s)	Temperature (ºC)	Operating temperature range (ºC)	Operating time range (s)
C1	15	100	100-125	15-30
C2	5	150	120-150	5-30
C3	15	150	120-150	5-30
C4	**0**	**25**	**only room temperature**	**-**
C5	15	210	200-225	5-60
C6	30	225	200-240	30-60
M1	30	125	125-150	15-30
M2	5	150	150	5-30

Table 3. Tribological and AFM measurements conditions for lubricating grease samples tested in a tribological contact

Grease samples	Tribological measurements conditions			AFM time–temperature sample preparation procedure applied	
	normal load (N)	rotational speed, (rpm)	time (min)	temperature (ºC)	time (s)
C5	40	400	12	210	15
	40	0.1-1000	10	210	5
C6	40	400	12	200	15
	40	0.1-1000	10	200	15
M1	40	400	12	125	30
	40	0.1-1000	10	125	30

Figure captions

Fig. 1. Influence of the temperature-time procedure applied on sample preparation for AFM imaging the microstructure of two lubricating greases: C5) a lithium complex grease and C6) a lithium calcium complex grease. (window sizes of 20 µm x 20 µm)

Fig. 2. Comparison between AFM (window sizes of 20 µm x 20 µm and 5 µm x 5 µm) and SEM (15-20kV and 200-5000X magnification) micrographs corresponding to the four anhydrous calcium soap-based greases studied (C1-C4).

Fig. 3. Comparison between AFM (window sizes of 20 µm x 20 µm and 5 µm x 5 µm) and SEM (20kV and 200-13000X magnification) micrographs corresponding to the lithium complex (C5) and lithium calcium complex soap (C6) greases.

Fig. 4. Comparison between AFM (window sizes of 20 µm x 20 µm and 5 µm x 5 µm) and SEM (15kV and 1000-13000X magnification) micrographs corresponding to model biopolymer-based greases: chemically modified methylcellulose- (M1) and lignocellulosic material (M2)-based greases.

Fig. 5. Effect of tribology testing on the morphology of samples C5, C6 and M1. Left side: fresh grease samples; right side: greases submitted to frictional tests, a) 40N at a constant speed of 400 rpm, and b) 40N and rotational speed sweep (0.1-1000 rpm) in a ball-on-plate tribocontact. (window sizes of 20 µm x 20 µm and 5 µm x 5 µm).

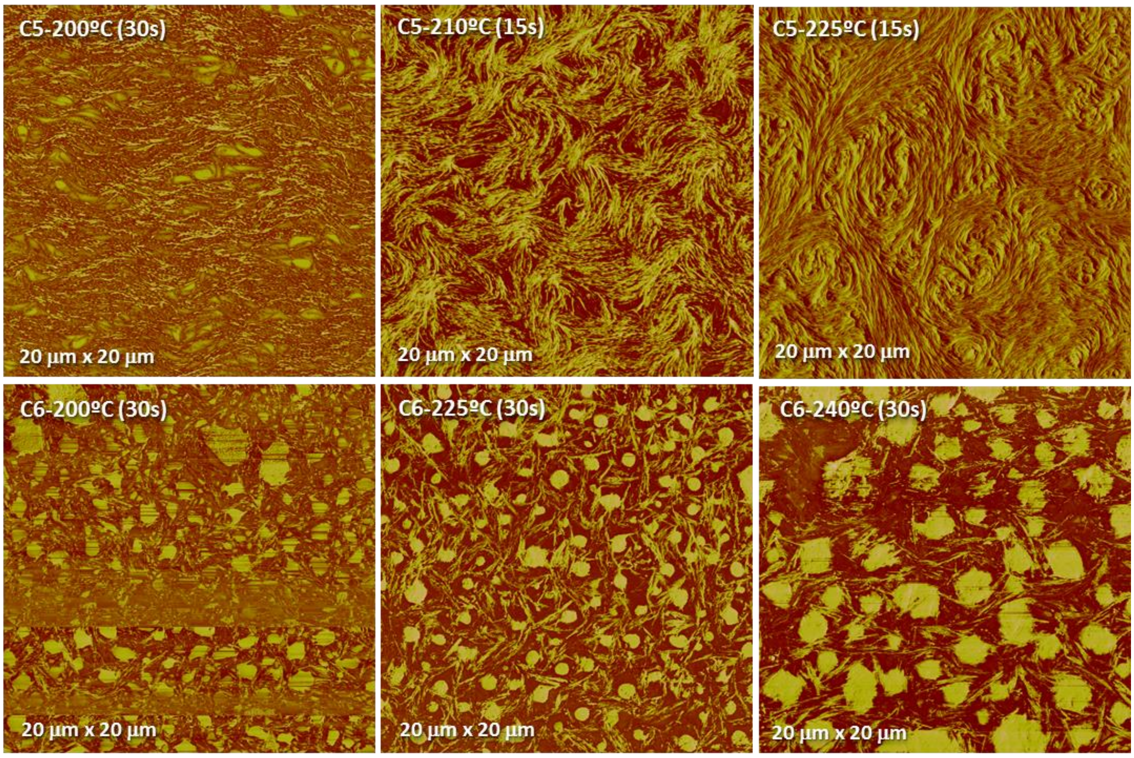
C5-200ºC (30s)
20 µm x 20 µm
C5-210ºC (15s)
20 µm x 20 µm
C5-225ºC (15s)
20 µm x 20 µm
C6-200ºC (30s)
20 µm x 20 µm
C6-225ºC (30s)
20 µm x 20 µm
C6-240ºC (30s)
20 µm x 20 µm

Fig.1.

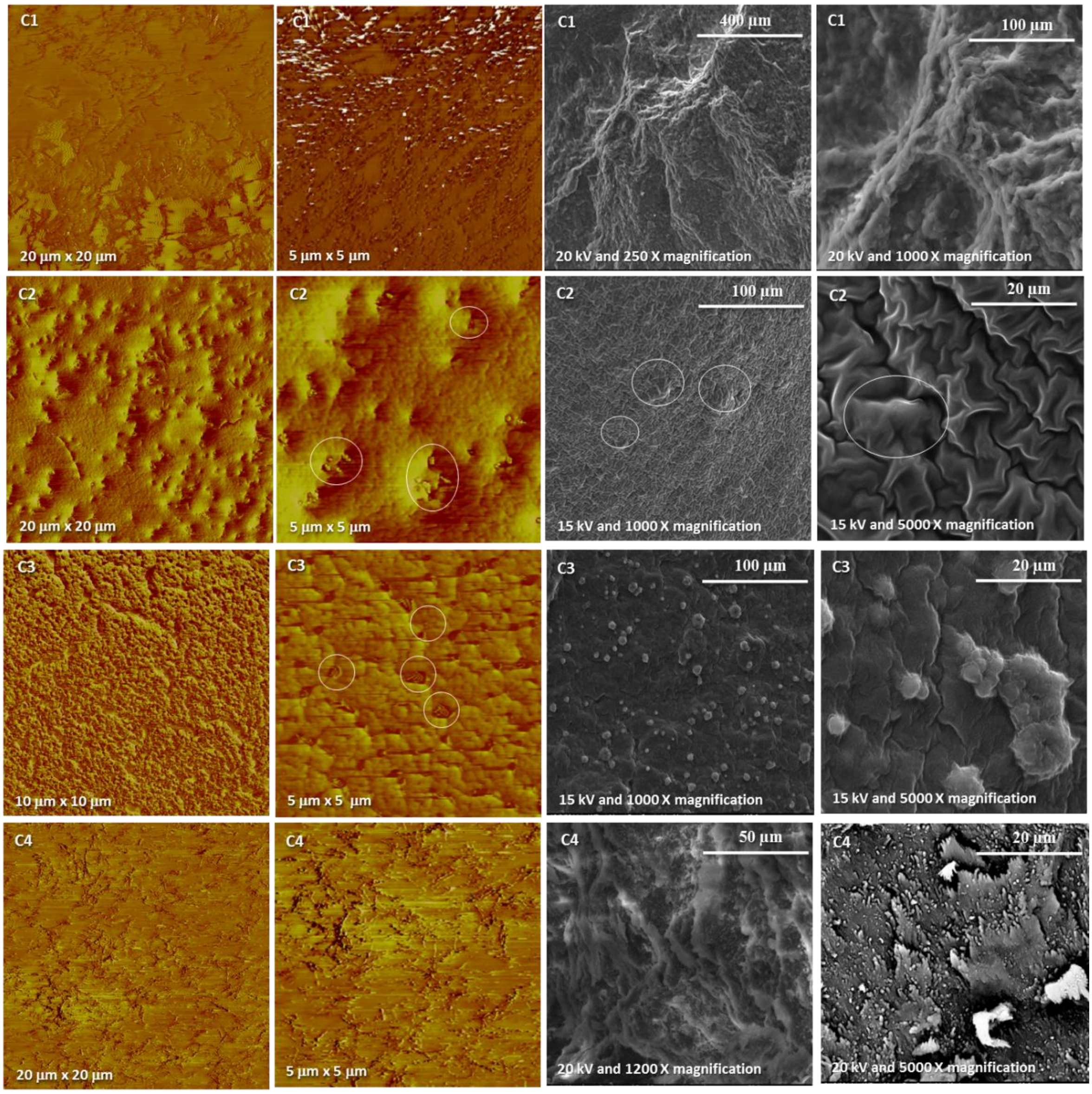
C1
20 µm x 20 µm
C1
5 µm x 5 µm
C1
400 µm
20 kV and 250 X magnification
C1
100 µm
20 kV and 1000 X magnification
C2
20 µm x 20 µm
C2
5 µm x 5 µm
C2
100 µm
15 kV and 1000 X magnification
C2
20 µm
15 kV and 5000 X magnification
C3
10 µm x 10 µm
C3
5 µm x 5 µm
C3
100 µm
15 kV and 1000 X magnification
C3
20 µm
15 kV and 5000 X magnification
C4
20 µm x 20 µm
C4
5 µm x 5 µm
C4
50 µm
20 kV and 1200 X magnification
C4
20 µm
20 kV and 5000 X magnification

Fig.2.

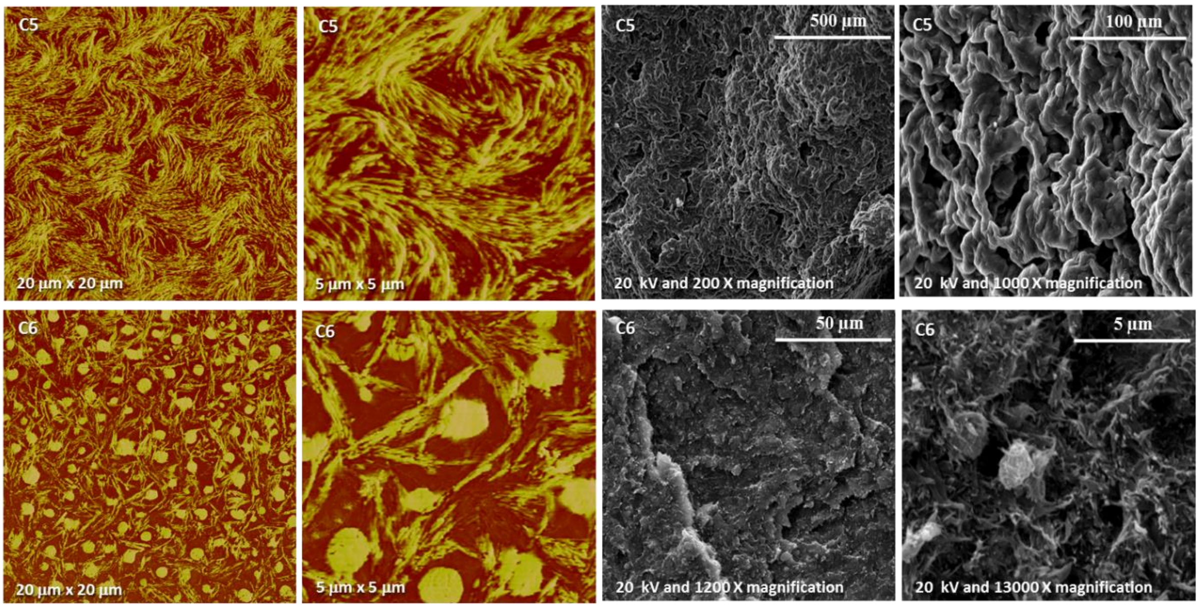
C5
20 µm x 20 µm
C5
5 µm x 5 µm
C5
500 µm
20 kV and 200 X magnification
C5
100 µm
20 kV and 1000 X magnification
C6
20 µm x 20 µm
C6
5 µm x 5 µm
C6
50 µm
20 kV and 1200 X magnification
C6
5 µm
20 kV and 13000 X magnification

Fig.3.

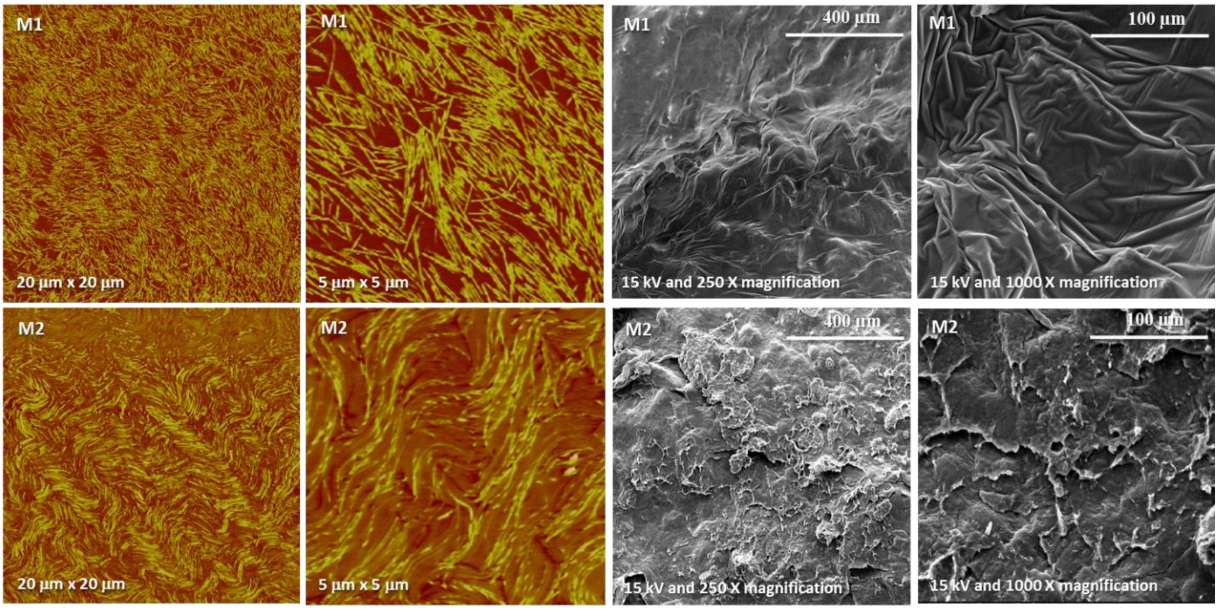
M1
20 µm x 20 µm
M1
5 µm x 5 µm
M1
400 µm
15 kV and 250 X magnification
M1
100 µm
15 kV and 1000 X magnification
M2
20 µm x 20 µm
M2
5 µm x 5 µm
M2
400 µm
15 kV and 250 X magnification
M2
100 µm
15 kV and 1000 X magnification

Fig.4.

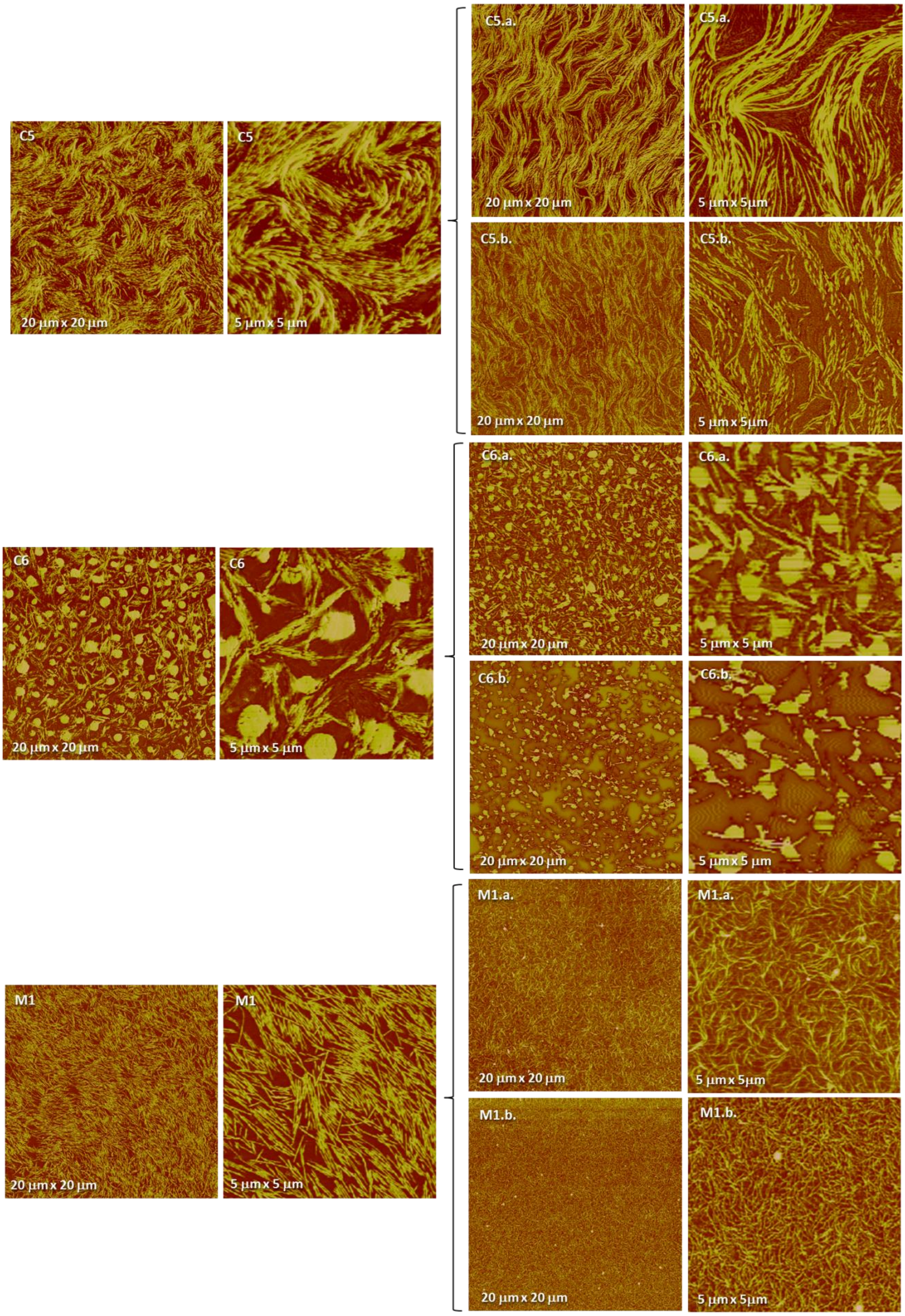
C5
20 µm x 20 µm
C5
5 µm x 5 µm
C5.a.
20 µm x 20 µm
C5.a.
5 µm x 5µm
C5.b.
20 µm x 20 µm
C5.b.
5 µm x 5µm
C6
20 µm x 20 µm
C6
5 µm x 5 µm
C6.a.
20 µm x 20 µm
C6.a.
5 µm x 5 µm
C6.b.
20 µm x 20 µm
C6.b.
5 µm x 5 µm
M1
20 µm x 20 µm
M1
5 µm x 5 µm
M1.a.
20 µm x 20 µm
M1.a.
5 µm x 5µm
M1.b.
20 µm x 20 µm
M1.b.
5 µm x 5µm

Fig.5.